# CORRECTION FOR SYSTEMATIC ERRORS OF A DRUM-TYPE SCANNING MICRODENSITOMETER

Dr. Paul R. Wolf, Professor
Mr. Bon A. Dewitt, Graduate Student
University of Wisconsin, Madison, Wisconsin
USA
Commission 3

## ABSTRACT

An evaluation of the systematic, geometrical errors of a Drum-Type scanning microdensitometer, and method of correcting for them is presented. In this research, reference holes were drilled, in a grid pattern, into the emulsion of several photographs prior to scanning. Photo coordinates of the reference marks were determined using a monocomparator, and for comparison, their positions were also extracted from the scanned image by computer processing. This processing included automatic recognition of the marks by image correlation followed by a minimally constrained transformation of raw scanner coordinates to the photo system. The transformed values show significant errors displaying a highly systematic shearing effect. After correcting for this effect, the distortions which remain show a pattern that is not systematic from one photo to the next. In an attempt to achieve a higher level of accuracy, these remaining distortions were modelled through a least squares fit of polynomials, resulting in scanner positions correct to within an RMS error of approximately one-fourth the pixel size.

## INTRODUCTION

Densitometric measurements have many applications in Photogrammetry and Remote Sensing. One photogrammetric application that has been emerging in recent years is in analytical aerotriangulation. In this procedure, scanning microdensitometers are used rather than comparators for determining photo image coordinates. Scanning microdensitometers measure variations in image density throughout a photo, resulting in a picture element representation, with positions specified in terms of scanner rows and columns. The row and column locations are subsequently transformed into the conventional x-y photo coordinate system for use in aerotriangulation equations.

In this type of aerotriangulation research at the University of Wisconsin-Madison, image density measurements have been obtained using a rotating drum, scanning microdensitometer. This research has indicated the presence of significant geometrical errors in the scanner system. To produce the highest level of accuracy in aerotriangulation, therefore, it is necessary to account for these systematic errors, which is the subject of this paper. It is recognized that rotating drum scanners were intended principally for Remote Sensing applications wherein extreme accuracy in pixel location is not necessarily of paramount concern. Nevertheless, by evaluating and correcting for the geometrical errors using procedures similar to those described herein, significant improvements in accuracy can be achieved, making the results suitable for aerotriangulation.

## PHOTOGRAPHIC MEASUREMENTS

Photography exposed with a calibrated Zeiss RMK 15/23 aerial camera having eight fiducial marks (corner and side) was used in this project. Black and

white panchromatic film was used, and 5 photos were selected for the test. Thirty-two holes of 250 micrometer diameter were drilled into each photo in a grid pattern using a Wild PUG IV point transfer instrument. The pattern covered the full 9-inch square format, and consisted of four columns with 8 holes in each column. A one-micrometer H. Dell Foster monocomparator was used to measure photo coordinates of all fiducial marks and drill holes. Using the calibrated coordinates of the fiducial marks, and a 6-parameter two-dimensional affine coordinate transformation, coordinates of the drill holes in the camera's conventional calibrated x-y system were obtained from the comparator measurements.

The photographs were then mounted on the microdensitometer, with columns aligned essentially parallel with the direction of drum rotation. This was done because previous research had indicated that systematic errors were greater in the scanner's column coordinates (direction of drum rotation) than in its row coordinates (direction of lead screw axis), thus better modelling of the larger errors could more likely be achieved. The photographs were scanned using a 50 micrometer pixel size. It was intended to scan the entire contents of each photo including all eight fiducial marks. However, the maximum sized photo that could be accommodated by the microdensitometer used in this project was just under 9-inches square. Since the photos were a full 9-inches square, it was impossible to mount the photos on the drum to ensure that the entire format, including all eight fiducial marks, would be scanned. The results showed that in fact, for each photo all drill holes were scanned, but some fiducials were missed. Nevertheless a sufficient number of fiducials was scanned to enable suitable completion of the investigation.

## EVALUATING THE SYSTEMATIC ERRORS

The first step in evaluating the systematic errors of the scanning system required that the row/column locations of the fiducials be determined. This was done automatically by computer using numerical image correlation techniques that included resampling. Initially, relatively large areas of search were probed in the generally expected locations of fiducials until two of them were found. Then a 4-parameter two-dimensional conformal coordinate transformation was performed to predict more precisely the row/column locations of the remaining fiducials, as well as all drill holes. This accurate prediction enabled correlation of the remaining fiducials and all drill holes at a significant savings in computer time. By using idealized image templates and resampling techniques, the correlated fiducial and drill hole positions could be located to accuracies at a sub-pixel level (Wolf and Dewitt, 1982).

After the row/column coordinates of the fiducials and drill holes had been obtained to sub-pixel level, the two fiducial marks that had the strongest correlation were used to transform all drill hole row/column locations into the calibrated photo coordinate system. This transformation involved no redundancy and consisted of only rotation and translation. A comparison of these x-y transformed drill hole photo coordinates to those measured with the monocomparator yielded positional discrepancies. Figure 1 illustrates both the x and y components of these discrepancies graphically for one representative photo, and columns 2 and 3 of Table 1 list their numerical values. From the figure and table it can be seen that discrepancies for this photo in y are considerably larger than those in x, and that they define a rather systematic shearing pattern. This was true for all photos evaluated. For the photo of Table 1, the maximum value in y was 328

Figure 1

Plot of Scanning Microdensitometer Positional Discrepancies for Photo No. 75.

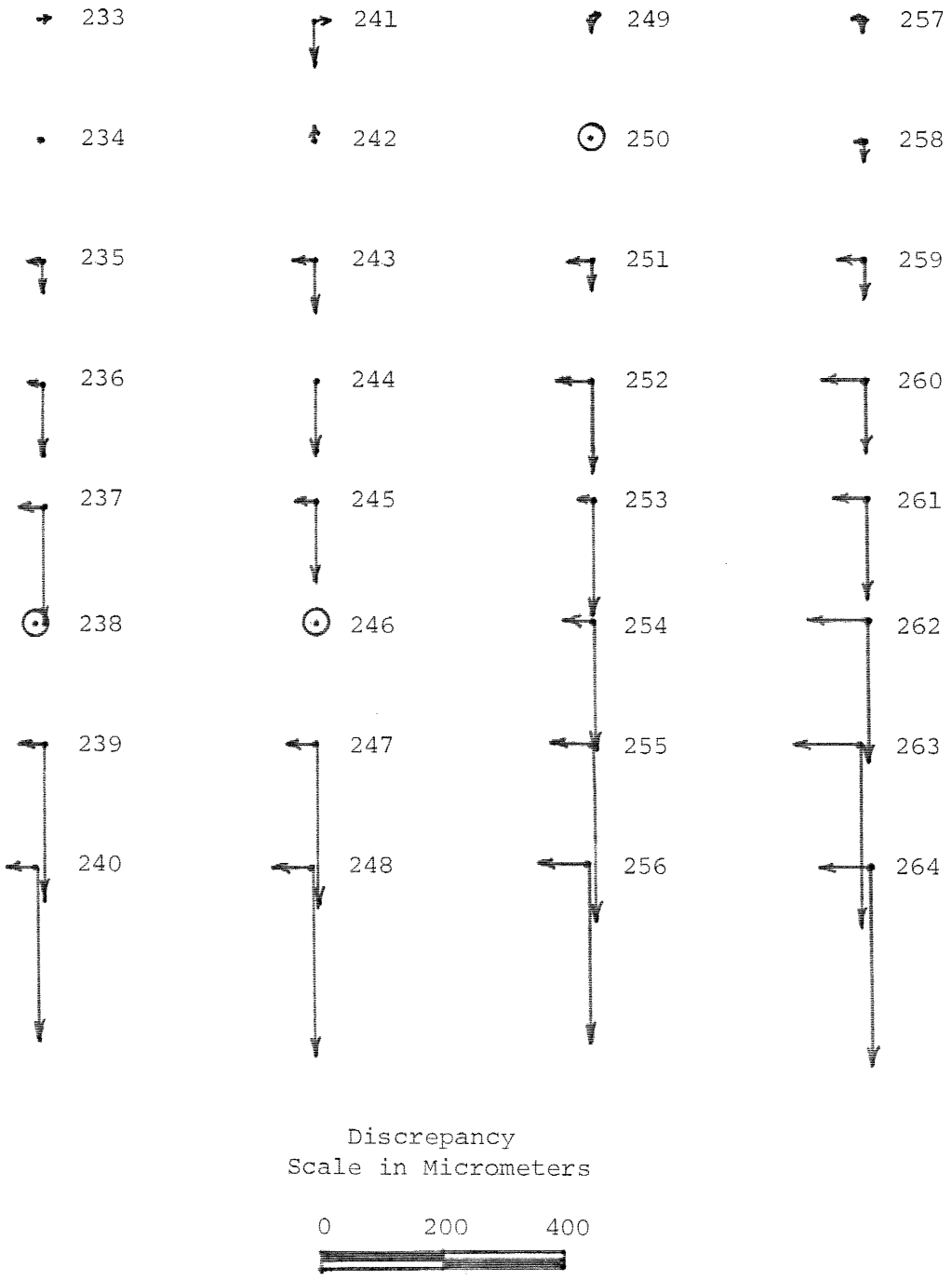

Table 1
Discrepancies in Scanner Coordinates in Micrometers
Photo No. 75 of Scanner Test

| Point No. | Discrepancies prior to Correction | | Discrepancies after Correction Eqs. No. 1 | | Discrepancies after Correction Eqs. No. 2 | | Discrepancies after Correction Eqs. No. 3 | |
|---|---|---|---|---|---|---|---|---|
| | x | y | x | y | x | y | x | y |
| (1) | (2) | (3) | (4) | (5) | (6) | (7) | (8) | (9) |
| 233 | + 19 | + 2 | + 1 | +14 | - 9 | - 4 | - 9 | - 3 |
| 234 | + 6 | 0 | + 3 | -31 | - 4 | -32 | - 6 | -14 |
| 235 | - 14 | - 44 | +13 | -32 | + 8 | -22 | + 7 | - 8 |
| 236 | - 12 | -120 | 0 | - 3 | - 3 | +14 | - 1 | +11 |
| 237 | - 30 | -191 | + 8 | +22 | + 7 | +40 | +12 | +19 |
| 239 | - 31 | -266 | -13 | + 5 | - 8 | +12 | - 4 | -15 |
| 240 | - 49 | -295 | - 5 | -13 | + 2 | -18 | 0 | -12 |
| 241 | + 23 | - 63 | -15 | +72 | -15 | +54 | -13 | +37 |
| 242 | - 1 | + 11 | - 1 | -47 | 0 | -51 | - 1 | -40 |
| 243 | - 34 | - 79 | +21 | - 4 | +22 | + 3 | +22 | +17 |
| 244 | + 5 | -120 | -28 | -10 | -26 | + 2 | -24 | + 7 |
| 245 | - 25 | -135 | -10 | -40 | - 6 | -28 | - 2 | -36 |
| 247 | - 49 | -277 | - 6 | +10 | - 1 | + 9 | + 4 | + 5 |
| 248 | - 68 | -314 | + 2 | 0 | + 8 | -14 | + 8 | +18 |
| 249 | + 11 | - 16 | -15 | +20 | - 9 | + 6 | -10 | -16 |
| 251 | - 29 | - 42 | + 4 | -47 | + 8 | -38 | + 2 | -24 |
| 252 | - 52 | -160 | +16 | +25 | +19 | +37 | +15 | +43 |
| 253 | - 19 | -198 | -27 | +17 | -25 | +28 | -26 | +22 |
| 254 | - 42 | -212 | -15 | -16 | -13 | -10 | -13 | -23 |
| 255 | - 68 | -301 | + 1 | +27 | + 2 | +23 | + 2 | +19 |
| 256 | - 88 | -292 | +10 | -28 | +10 | -47 | + 6 | -18 |
| 257 | - 12 | - 20 | - 3 | +17 | + 4 | +12 | + 7 | + 6 |
| 258 | - 16 | - 29 | -10 | -20 | - 6 | -14 | - 9 | + 7 |
| 259 | - 44 | - 62 | + 7 | -33 | + 9 | -19 | + 5 | + 4 |
| 260 | - 65 | -119 | +18 | -22 | +17 | - 5 | +15 | + 4 |
| 261 | - 41 | -170 | -17 | -18 | -20 | - 3 | -20 | -12 |
| 262 | - 83 | -232 | +15 | - 2 | +10 | + 7 | +12 | -16 |
| 263 | -110 | -308 | +31 | +28 | +23 | +25 | +26 | + 4 |
| 264 | - 86 | -328 | - 4 | + 2 | -14 | -18 | -15 | -13 |
| RMS | 48 | 193 | 14 | 27 | 13 | 24 | 12 | 18 |

micrometers, and the RMS value was 193 micrometers. In x the maximum value was 88 micrometers, and its RMS value was 48 micrometers. In Figure 1, three drill holes are circled. These were rejected from the analysis due to their weak correlation peaks.

## MODELLING THE DISCREPANCIES

The next step was to attempt to model the distortions, and this was done using polynomials. Three different types of polynomials of varying degree were tested and are given below. Equations No. (1) are a set of polynomials of degree one. This is the standard form for a six-parameter affine transformation. Here x and y are the coordinates determined from comparator measurement, X and Y are the coordinates determined from automated image correlation after rotation and translation into the calibrated fiducial system, and the A's and B's are coefficients to be determined.

$$\begin{aligned} x &= A_1 + A_2X + A_3Y \\ y &= B_1 + B_2X + B_3Y \end{aligned} \qquad (1)$$

Equations No. (2) are second degree polynomials. In these equations the notation is the same as that for the first degree equations.

$$\begin{aligned} x &= A_1 + A_2X + A_3Y + A_4X^2 + A_5Y^2 + A_6XY \\ y &= B_1 + B_2X + B_3Y + B_4X^2 + B_5Y^2 + B_6XY \end{aligned} \qquad (2)$$

Equations No. (3) are polynomials of the third degree. Their notation is also the same as in the previous equations.

$$\begin{aligned} x &= A_1 + A_2X + A_3Y + A_4X^2 + A_5Y^2 + A_6XY + \\ &\quad A_7X^2Y + A_8XY^2 + A_9X^3 + A_{10}Y^3 \\ y &= B_1 + B_2X + B_3Y + B_4X^2 + B_5Y^2 + B_6XY + \\ &\quad B_7X^2Y + B_8XY^2 + B_9X^3 + B_{10}Y^3 \end{aligned} \qquad (3)$$

For each of these sets of polynomials, observation equations were written and a least squares solution made for the unknown A's and B's. In the process, residuals representing the misfit of the equations to the data set were determined. The results of this polynomial curve fitting are given in Table 1 for the selected representative photo. Columns 4 and 5 list the residual discrepancies in x and y, respectively, for the first degree polynomial, [Equations (1)]. Columns 6 and 7 give the residual discrepancies in x and y, respectively, for the second degree polynomial, [Equations No. (2)], and columns 8 and 9 tabulate the residual discrepancies in x and y, respectively, for the third degree polynomials, [Equations No. (3)]. The bottom row gives RMS discrepancy values for each column.

## CONCLUSIONS

Several conclusions can be drawn from this and other related research conducted at the University of Wisconsin, Madison.

(1) The results of this experiment confirm preliminary research findings which indicated that the scanner introduces significant distortions, especially in its less stable direction of drum rotation.

(2) First degree polynomials provide about the same quality of correction to the x coordinates as those of third degree. This is indicated by the RMS values in columns 4, 6 and 8 of Table 1 where the x residuals are approximately the same for all three polynomials. This shows that the distortion pattern in the x (lead screw direction) is less complicated than that in the y (drum rotation direction).

(3) For higher degree polynomials the x rms values approach 12 micrometers which corresponds to approximately one-fourth of the pixel size. This would tend to indicate the ultimate accuracy to which coordinates of discrete images can be determined by correlation in the scanned image, which was also concluded from previous research.

(4) Higher degree polynomials improve accuracy in y coordinates, as shown by the data of Table 1. This indicates that a larger, more complicated distortion pattern exists in this direction. The RMS value of 18 micrometers for corrected y coordinates is only slightly greater than one-fourth the pixel size and indicates that most, but not all, positional distortion has been removed.

(5) Although data is shown for only one representative photo, examination of the results of all others tested revealed that y distortions were consistently greater than those in x but no specific pattern of distortions was repeated from photo to photo. From this it is concluded that distortion corrections must be made independently for each photo. The technique presented in this paper of making drill holes and measuring their coordinates by comparator requires much more additional human operation than is desirable in an automated mapping system. Thus a more practical approach would be to employ photography taken with a reseau camera wherein the distortion corrections can be computed and applied automatically for each photo.

## REFERENCES

1. Forsythe, G.E., M.A. Malcolm and C.B. Moler: "Computer Methods for Mathematical Computations," Prentice-Hall, Inc., Englewood Cliffs, N.J., 1977.
2. Wolf, P.R.: "Elements of Photogrammetry," 2nd Ed., McGraw-Hill Book Co., Inc., New York, 1983.
3. Wolf, P.R. and B.A. Dewitt: "An Automated Photogrammetric Mapping System," Proceedings of ISPRS Commission IV Symposium, Crystal City, Va., 1982.